1521-0103/382/3/287–298$35.00
THE JOURNAL OF PHARMACOLOGY AND EXPERIMENTAL THERAPEUTICS

dx.doi.org/10.1124/jpet.122.001151
J Pharmacol Exp Ther 382:287–298, September 2022

The Journal of PHARMACOLOGY And Experimental Therapeutics

Pharmacological Evaluation of a Pegylated Urocortin-1 Peptide in Experimental Autoimmune Disease Models[S]

Josef G. Heuer, Catalina M. Meyer, Hana E. Baker, Andrea Geiser, Jonathan Lucchesi, Daniel Xu, Matthew Hamang, Jennifer A. Martin, Charlie Hu, Kenneth D. Roth, Kannan Thirunavukkarasu, Jorge Alsina-Fernandez, and Yanfei L. Ma

Lilly Research Laboratories, Eli Lilly and Company, Lilly Corporate Center, Indianapolis, Indiana

Received February 4, 2022; accepted May 25, 2022

ABSTRACT

Urocortin-1 (UCN1) is a member of the corticotropin releasing hormone (CRH) family of peptides that acts through CRH-receptor 1 (CRHR1) and CRH-receptor 2 (CRHR2). UCN1 can induce the adrenocorticotropin hormone and downstream glucocorticoids through CRHR1 and promote beneficial metabolic effects through CRHR2. UCN1 has a short half-life and has been shown to improve experimental autoimmune disease. A pegylated UCN1 peptide (PEG-hUCN1) was generated to extend half-life and was tested in multiple experimental autoimmune disease models and in healthy mice to determine effects on corticosterone induction, autoimmune disease, and glucocorticoid induced adverse effects. Cardiovascular effects were also assessed by telemetry. PEG-hUCN1 demonstrated a dose dependent 4–6-fold elevation of serum corticosterone and significantly improved autoimmune disease comparable to prednisolone in several experimental models. In healthy mice, PEG-hUCN1 showed less adverse effects compared with corticosterone treatment. PEG-hUCN1 peptide induced an initial 30% reduction in blood pressure that was followed by a gradual and sustained 30% increase in blood pressure at the highest dose. Additionally, an adeno-associated viral 8 (AAV8) UCN1 was used to assess adverse effects of chronic elevation of UCN1 in wild type and CRHR2 knockout mice. Chronic UCN1 expression by an AAV8 approach in wild type and CRHR2 knockout mice demonstrated an important role of CRHR2 in countering the adverse metabolic effects of elevated corticosterone from UCN1. Our findings demonstrate that PEG-hUCN1 shows profound effects in treating autoimmune disease with an improved safety profile relative to corticosterone and that CRHR2 activity is important in metabolic regulation.

SIGNIFICANCE STATEMENT

This study reports the generation and characterization of a pegylated UCN1 peptide and the role of CRHR2 in UCN1-induced metabolic effects. The potency/selectivity, pharmacokinetic properties, pharmacodynamic effects, and efficacy in four autoimmune models and safety profiles are presented. This pegylated UCN1 shows potential for treating autoimmune diseases with reduced adverse effects compared to corticosterone treatment. Continuous exposure to UCN1 through an AAV8 approach demonstrates some glucocorticoid mediated adverse metabolic effects that are exacerbated in the absence of the CRHR2 receptor.

Introduction

The CRH family of peptides are structurally similar and include CRH, UCN1, UCN2, and UCN3 (Squillacioti et al., 2019). These peptides modulate the stress response in vertebrates through their actions on two G-protein coupled receptors, CRHR1 and CRHR2, which are coupled to the cAMP/Protein kinase A pathway (Grammatopoulos and Ourailidou, 2017). Although these peptides were originally noted for their cardiovascular properties (Walczewska et al., 2014), they have also demonstrated metabolic and immunomodulatory effects (Asakawa et al., 1999; Jamieson et al., 2011; Souza-Moreira et al., 2011; Gao et al., 2016; Borg et al., 2019). Cardiovascular and beneficial metabolic actions of these peptides, including acute reductions in food intake, are driven through activation of the CRHR2 receptor, which is expressed in the hypothalamus and peripheral tissues such as skeletal muscle, heart, and the vasculature (Lovenberg et al., 1995; Hashimoto et al., 2004). The endocrine effects on the hypothalamic pituitary adrenal axis are driven mainly by the activation of the CRHR1 receptor in the anterior pituitary, resulting in release of adrenocorticotropin (ACTH) and subsequent glucocorticoid production in the adrenal glands (Papadimitriou and Priftis, 2009).

UCN1, a potent nonselective CRH receptor ligand, has been shown to elevate plasma ACTH and cortisol in healthy human volunteers (Davis et al., 2004). UCN1 has also been shown to attenuate disease in experimental murine autoimmune models, including trinitrobenzenesulfonic acid induced colitis and collagen induced arthritis (Gonzalez-Rey et al., 2006a, 2007),

This study received no external funding and was funded by Eli Lilly and Company Inc.
All authors are current employees of Eli Lilly and Company Inc. and may own stock in the company.
dx.doi.org/10.1124/jpet.122.001151.
[S] This article has supplemental material available at jpet.aspetjournals.org.

ABBREVIATIONS: AAV8, adeno-associated virus serotype 8; ACTH, adrenocorticotropin; BMD, bone mineral density; CFA, complete Freund's adjuvant; CRH, corticotropin releasing hormone; CRHR1, CRH-receptor 1; CRHR2, CRH-receptor 2; EAE, encephalomyelitis; HEC, hydroxyethyl cellulose; IMQ, imiquimod; KO, knockout; PEG, pegylated; PO, by mouth; QD, once daily; UCN1, urocortin-1; WT, wild type.

as well as rat experimental autoimmune encephalomyelitis (EAE) (Poliak et al., 1997). In addition, UCN1 has been shown to be protective in experimental lethal endotoxemia by downregulating the inflammatory response (Gonzalez-Rey et al., 2006b). Mechanistically, UCN1 has been suggested to reduce inflammation by i) suppression of cytokine production tumor necrosis factor-alpha, interleukin-1 beta, interleukin-6, interleukin-12, interferon-gamma, macrophage inflammatory protein-2, and regulated upon activation, normal T cell expressed and presumably secreted); ii) suppression of Th1 and Th17 driven responses; and iii) generation or activation of Treg cells in vivo (Gonzalez-Rey et al., 2006a, 2006b). CRH receptors are present on immune cells, including macrophages, granulocytes, monocytes, B-cells, and T-cells (Webster et al., 1990; Radulovic et al., 1999; Dermitzaki et al., 2018; Harlé et al., 2018). UCN1 has been shown to have both pro- and anti-inflammatory effects, including promotion of mast cell degranulation (Singh et al., 1999); yet it has also been shown to suppress lipopolysaccharide induced tumor necrosis factor-alpha release from macrophages (Tsatsanis et al., 2007) and promote macrophage apoptosis (Tsatsanis et al., 2005). Although CRH receptors have been reported on T-cells (Singh and Fudenberg, 1988), the direct effects of UCN1 on T-cells have not been thoroughly investigated. Since UCN1 can induce ACTH release through CRHR1 stimulation in the pituitary gland (Davis et al., 2004; Rademaker et al., 2005), it is possible that UCN1 can improve autoimmune disease indirectly via glucocorticoid effects on immune cells. Glucocorticoids have potent anti-inflammatory effects on immune cells, have been widely studied, and are a mainstay of therapy for most autoimmune diseases. Most in vivo studies reporting beneficial effects of UCN1 treatment in autoimmune disease models failed to characterize the effects of UCN1 on corticosterone production, although one study reported beneficial effects of CRH in an adrenalectomized rat EAE model, suggesting an involvement of both direct and indirect effects of CRH on disease outcome (Poliak et al., 1997).

The native UCN1 peptide tested in all reported experimental models of autoimmune disease was 40 amino acids in length and dosed by daily injection. Although there are no reported pharmacokinetic studies of UCN1 in rodents to our knowledge, the pharmacokinetic properties of UCN1 in humans and sheep indicate that UCN1 has a short half-life of 1 to several hours, respectively (Davis et al., 2004; Patel et al., 2012). The use of a long acting UCN1 peptide would make clinical testing of UCN1 more reasonable, yet would be expected to chronically elevate endogenous glucocorticoids, which have well known adverse effects that could negate the beneficial effects of this type of therapy in patients with autoimmune diseases. Unlike CRH, UCN1 is a potent agonist at the CRHR2 receptor, which has been shown to impart beneficial metabolic properties that might be able to counter the adverse effects of elevated glucocorticoids. The potential of a pegylated UCN1 peptide to improve autoimmune disease and overcome the adverse metabolic effects of glucocorticoid induction has not been previously tested.

Materials and Methods

Peptides. Native human/rat CRH (Cat. No. AS-24254) was obtained from Anaspec (Fremont, CA) and native human UCN1 peptide (Cat. No. H37700.05) was obtained from Bachem (Torrance, CA). Human UCN2 peptide and a modified version of human UCN1 peptide were synthesized. Modifications to human UCN1 peptide included replacement of the human sequences from aa 21–28 with the homologous frog sauvagine sequence "EKQEKEKQ" to reduce binding to CRH binding protein (Isfort et al., 2006) and insertion of a Cysteine residue at position 31 for pegylation. The amino acid sequence of the PEG-hUCN1 peptide is DNPSLSIDLTFHLLRTLLELEKQEKEKQQA C(PEG20 acetamide)QNRIIFDSV-NH2. Peptides were synthesized by solid-phase peptide synthesis with established Fmoc/tBu protocols. Specifically, an automated peptide synthesizer was used (Symphony from Protein Technologies Inc., Tucson, AZ). Rink Amide AM was the starting resin to generate the corresponding C-terminal amide peptide, and couplings were mediated by diisopropylcarbodiimide/Oxyma in dimethyl formamide with 5-fold excess of reagents. After final cleavage of the peptide from the solid support, peptides were purified using reversed-phase chromatography. Purified fractions were pooled and lyophilized to generate peptide powders as trifluoroacetate salts. Peptides were characterized by laser capture/mass spectrometry. Elongation of peptide half-life in vivo was accomplished by conjugation in solution of the peptide to a 20 kDa functionalized polyethylene glycol polymer. One molar equivalent of mPEG-20 kDa iodoacetamide [CH3-O-(CH2-CH2-O)n-(CH2)3-NH-CO-CH2-I] (NOF Sunbright ME-200IA) was used in the derivation of Cys sidechain at position 31 using aqueous buffer (0.1M bicarbonate/carbonate, pH8.0, 10mM EDTA):acetonitrile (2:1; v/v). The reaction mixture was purified using reversed-phase chromatography.

In Vitro Cell Based Assays. The mouse CRHR1 (Cat. No. 93-0473E2) and human CRHR2 (Cat. No. 93-0251E2) PathHunter eXpress beta arrestin cell-based assays were purchased from Eurofins/DiscoverX (Fremont, CA) and run according to their instructions. The data were imported to, analyzed, and graphed with GraphPad Prism v.8.0 software.

Peptide Pharmacokinetics. The pharmacokinetics of PEG-hUCN1 peptide were characterized in healthy female C57BL/6J mice (Envigo Inc., Indianapolis, IN) at 6–7 weeks of age on Purina 5001 diet. The exposure of peptide equivalent concentrations of PEG-hUCN1 peptide was assessed from plasma using a laser capture/mass spectrometry bioanalytical method in which N-terminal and C-terminal peptide mass, generated by tryptic digestion, were monitored. The study was dosed in peptide equivalent weight doses, and circulating concentrations were expressed in peptide equivalent concentrations. Pharmacokinetic parameters were calculated by noncompartmental analysis using Phoenix WinNonlin Version 8.1. All reported pharmacokinetic parameters were based on the N-terminal peptide concentrations.

Mouse Studies. All animal work followed protocols approved by the Eli Lilly and Company Animal Care and Use Committee. All animal studies were conducted in accordance with the American Association for Laboratory Animal Care institutional guidelines. Unless stated otherwise, mice were acclimated for a minimum of 5 days prior to experiments and were housed two to three per cage in high density racks, sawdust bedding, and nestlets with Purina 2014 or 2008 diet and water bottles. Animals in nondisease models were randomized into groups by body weight. Vehicle for subcutaneous injections was 0.9% physiologic saline.

Pharmacodynamic Studies and Measurement of Corticosterone. PEG-hUCN1 was studied in both single and repeat dose studies with female C57BL/6J mice (Jackson Laboratories, Bar Harbor, ME) at different ages. In some experiments comparisons were made to corticosterone administered in the drinking water at 100 mcg/ml (Gasparini et al., 2016), which was made fresh once weekly. Corticosterone (Sigma-Aldrich, St. Louis, MO; Cat. No. 27840) was first dissolved in 100% Ethanol at 10 mg/ml and then diluted with water to 1% Ethanol. All other groups of mice received 1% Ethanol in the drinking water. For measurement of serum corticosterone, blood drops obtained by tail stick were collected onto Whatman FTA DMPK-C dried blood spot cards (GE Healthcare Life Sciences, Piscataway, NJ; Cat No. WB129243). Baseline corticosterone values were

determined at 8–9 AM prior to administration of peptides. Animals were handled for several days prior to experiments to acclimate them to the procedure. Mice were dosed with physiologic saline or peptide at several dose levels subcutaneously either as a single dose or as multiple doses at defined time intervals, and blood drops obtained by tail stick were collected onto dried blood spot cards at defined time intervals for measurement of corticosterone. Corticosterone was measured by liquid chromatography-tandem mass spectrometry with Shimadzu LC-20AD HPLC pumps, Shimadzu CBM-20A HPLC controller, Shimadzu SIL-20A autosampler (Shimadzu Scientific Instruments, Inc., Columbia, MD), and a Sciex API 6500 mass spectrometer (Sciex, Inc., Framingham, MA). Calibration curves were prepared using corticosterone (Sigma-Aldrich, St. Louis, MO; Cat. No. 46148) in control human plasma with EDTA (Bioreclamation, Inc., New Cassel, NY), pipetted onto dried blood spot cards (GE Healthcare, Chicago, IL; Cat. No. WB129243) and dried overnight in a desiccator. Punches (3 mm diameter) of all samples and standards were extracted in methanol containing d8-costicosterone (Cambridge Isotope Laboratories, Tewksbury, MA; Cat. No. DLM-7347), dried under heated nitrogen, and reconstituted in 50 μl of 10% methanol. Injections (20 μl) were separated with an XBridge C18 column (Waters Corp., Milford, MA, 2.1x50 mm, 3.5 μm, Cat No. 186003021) at room temperature with a flow rate of 1 ml/min and an isocratic mobile phase of 25% acetonitrile/75% water/0.1% formic acid. Tandem mass spectrometry analysis used positive heated electrospray at 375°C in Multiple Reaction Mode.

Imiquimod Induced Skin Inflammation Model. Female BALB/c mice (Envigo, Inc., Indianapolis, IN) at 8 weeks of age were maintained on a 12 hr light/dark cycle at 22°C with ad lib access to food (Certified Rodent Diet #2014C) and water. Thirty mg of 3.75% imiquimod (IMQ) cream (Zyclara) (Bausch Health Companies Inc., Laval, Quebec, Canada) was applied daily to the shaved back (2 x 2 cm region) of mice. Mice were randomized based on body weight into treatment groups with eight mice in each group. PEG-hUCN1 at 0.03 or 1 mg/kg in PBS was given subcutaneously at 2 days before IMQ and again at 3 days post IMQ application. Prednisolone (Sigma-Aldrich, St. Louis, MO; Cat. No. P6004) at 10 mg/kg in 1% hydroxyethyl cellulose (HEC) vehicle was given by oral gavage daily as the positive control. Two groups of IMQ mice were dosed with either PBS or 1% HEC as the vehicle controls for the respective compound. Mice were weighed and scored daily. Clinical scores were given 0–4 based on none, slight, moderate, marked, or severe on erythema, thickness, and scaling changes with 12 being the maximal sum score. All mice were sacrificed on day 8 and a 1 cm skin sample was taken for histopathological evaluation. Formalin-fixed skin samples were trimmed, routinely processed, paraffin-embedded, microtomed at a thickness of 5μm, and stained with hematoxylin and eosin. Tissue sections were examined by light microscopy and graded for disease parameters by a board-certified veterinary pathologist blinded to the treatment groups. The histology sum score had a total possible score of 11. Individual scores included inflammation (0–5), epidermal hyperplasia (0–5), and hyperkeratosis (0 or 1) from normal or absent as the lowest score to severe as the highest score.

Collagen-Induced Arthritis Model. Male, 6–7 weeks old DBA/1 mice (Envigo, Inc., Indianapolis, IN) with a mean body weight of 19–22 g were used for the study. Animals were fed with TD2014 diet and provided water ad libitum. Immunization emulsion was prepared with 2 mg/ml bovine collagen-II mixed with an equal volume of complete Freund's adjuvant (CFA). Mice were immunized intradermally with 100 ul of collagen emulsion in two sites each at the base of the tail on day 1 and again on day 21. Animals were randomized based on the paw score and body weight on day 27 into study groups with 10 mice in each group. PEG-hUCN1 at 0.03 or 0.1 mg/kg in PBS was given subcutaneously every 5 days starting on day 28. Prednisolone (Sigma-Aldrich, St. Louis, MO; Cat. No. P6004) was dosed by oral gavage once daily at 10 mg/kg as the positive control. Two groups of collagen induced arthritis mice were dosed with either PBS or 1% HEC as the respective vehicle controls. Clinical scores were given 0–5 based on the arthritis severity in all four paws with 20 being the maximal sum score for each mouse. All mice were sacrificed on day 42 and paws were taken for histopathological evaluation and prepared according to standard procedures. Tissue sections were stained with H&E or toluidine blue and examined by light microscopy and graded for disease parameters by a board-certified veterinary pathologist blinded to the treatment groups.

Proteolipid Protein Induced Remitting-Relapsing EAE Model. Female 9–10-week-old Swiss Jim Lambert (SJL) mice (Jackson Laboratories) with a mean body weight of 18–21 g were used for the study. Animals were fed with TD2014 diet and provided water ad libitum. Mice were immunized by shallow subcutaneous injections of four 50 ul each on the back with the Hooke Kit proteolipid protein 139-151/CFA Emulsion (catalog number EK-0120, Hooke Laboratories, Lawrence, MA). On Day 12 after immunization, mice were assigned to one of the experimental groups, being populated with mice with and without clinical signs of EAE in a balanced manner. There were 15 mice in each group. PEG-hUCN1 at 0.03 or 0.1 mg/kg in PBS was given subcutaneously every 5 days starting on day 12. Prednisolone (Sigma-Aldrich, St. Louis, MO; Cat. No. P6004) at 10mg/kg in 1% HEC vehicle was given by oral gavage daily as the positive control. Clinical scores were collected daily from Day 9 until the end of the study at day 42. EAE scores were assigned on a scale 0–5 in 0.5-unit increments. Spinal cords were taken for histopathological evaluation and prepared according to standard procedures. Tissue sections were stained with Luxol fast blue-H&E staining and examined by light microscopy and graded for disease parameters by a board-certified veterinary pathologist blinded to the treatment groups.

MRL Lpr Lupus Nephritis Model. Female 14-week-old Murphy Roths Large Lymphoproliferative (MRL lpr) (JAX Stock No: 000485) and Murphy Roths Large (MRL MpJ) (JAX Stock No: 000486) mice (Jackson Laboratories, Inc. Bar Harbor, ME) were used for the study. Body weight and a spot urine sample for albumin/creatinine measurement from all MRL/lpr mice were obtained the week prior to treatment on day -3. Spot urine collections were done by placing mice on top of a 96-well polypropylene microplate to collect their urine over 2 hours. MRL lpr mice were randomized into equivalent groups of 10 by body weight and urine albumin/creatinine ratio on day 0. Vehicle (PBS) or PEG-hUCN1 peptide was dosed subcutaneously at 0.1 mg/kg on the left flank every 4 days. Body weight was measured on days 5 and 12, whereas urine albumin/creatinine ratio by spot collection was measured on day 12. Blood was collected by tail vein for corticosterone measurement at 6 hours post each dose over the 13-day study. On day 13 a necropsy was conducted, and spleens were removed and weighed. Blood was taken by the retro-orbital route under isoflurane anesthesia, and serum was obtained for analysis of blood urea nitrogen (BUN), Creatinine, and Globulins. Serum markers, urine albumin, and creatinine were determined on a Roche Hitachi Modular Analytics P analyzer with reagents from Roche (Roche, Indianapolis, IN).

AAV8 Murine UCN1 Model. AAV8 mouse UCN1 (Cat. No. AAV-275569; Titer 2.4×10^{13} gcu/ml) and AAV8 null (Cat. No. 7077; Titer 2.9×10^{13} gcu/ml) were purchased from Vector Biolabs (Malvern, PA) and administered intravenously as a single dose via the retro-orbital route under 3% isoflurane anesthesia to female C57Bl/6J mice aged 5-6 weeks (Jackson Laboratories, Bar Harbor, ME) at dose levels ranging from 1×10^9 to 5×10^{11} gcu/mouse. In a separate experiment, AAV8 mouse UCN1 at 1×10^{11} gcu/mouse was compared with corticosterone given in the drinking water at 100 mcg/ml on adverse effects in healthy female C57BL/6J mice at 5–6 weeks of age over a period of 4 weeks. AAV8 null at 1×10^9 gcu/mouse was used as the control. In another experiment, female B6;129 wild type (WT) or CRHR2 knockout (KO) (B6;129-Crhr2 < tm1Jsp>/J,) mice aged 11–12 weeks (Jackson Laboratories, Bar Harbor, ME) were administered a single intravenous dose of AAV8 null (1×10^9 gcu/mouse) or AAV8 mouse UCN1 (1×10^{11} gcu/mouse) by the retro-orbital route under 3% isoflurane anesthesia. Mice were monitored for up to 4 weeks.

Blood Pressure Telemetry. Female C57BL6/6NCrl mice aged 15–16 weeks of age were purchased from Charles River Laboratories

(Stone Ridge, NY) and received at Covance (Greenfield, IN) and implanted with HD-X11 transmitters from Data Science International (St. Paul, MN) for collection of blood pressure and heart rate data. After transmitter implantation, mice were single housed and provided standard chow and water ad libitum. Vehicle was dosed subcutaneously in all mice at 24 hours prior to dosing of peptides to collect control blood pressure and heart rate data. Human UCN1 at 0.1 mg/kg or PEG-hUCN1 at 0.3 or 1 mg/kg were dosed subcutaneously, then blood pressure and heart rate were recorded continuously for 96 hours.

Ex Vivo Micro-Computed Tomography Bone Analysis. Femurs were analyzed by quantitative micro-computed tomography using an LTC-100 CT scanner (Aloka, Wallingford, CT). Scans of the femora were taken at 0.4 and 4.4 mm from the end of the growth plate for distal metaphysis and midshaft analyses, respectively. Bone mineral content and bone area were obtained using Aloka software (SYS-C320 version 1.5); bone mineral density (BMD) was then calculated as bone mineral content normalized to bone volumetric area.

Analysis of Body Weight, Tissue Weights, Thymic Cell Counts, Food Intake, qNMR Body Composition, Glucose, and Total Cholesterol. Body weight and tissue weights were determined with balances from Mettler-Toledo Incorporated (Ballwin, MO). For thymic cell counts, the thymus was dissociated into a single cell suspension by gentle manual maceration and filtration through a 100-micron cell filter. The cell suspension was then counted on a ViCell cell counter (Beckman Coulter, Brea, CA). Food intake was measured daily or weekly by weighing the food placed in the cage at the beginning and end of the time period with a Mettler-Toledo Balance to get the amount consumed per day or week, typically for two to three mice housed per cage. The quantitative nuclear magnetic resonance (qNMR) measurements were collected using the EchoMRI whole body composition analyzer, version 200102 (System ID EMR-166-M) (EchoMRI, Houston, TX). Alert mice were placed into the appropriately sized qNMR restraint tube and secured with a tube plunger (one mouse at a time). The tube was placed into the qNMR machine, and the scan protocol was run. Scan duration was 2–3 minutes for each animal. Mice were promptly released from the scan tube back into their home cage once the scan was complete. For blood glucose, blood (30–50 μl) was obtained from the tail vein and dropped onto a Precision PCx blood glucose sensor electrode strip for blood glucose determination with a MediSense Precision PCx glucometer (Abbott Laboratories, Abbott Park, IL). Blood was collected from the retro-orbital sinus at the end of each study under isoflurane anesthesia. The clotted blood was centrifuged to obtain serum. Serum was analyzed for glucose or total cholesterol on a Roche Hitachi Modular Analytics P analyzer with reagents from Roche (Indianapolis, IN).

Statistical Analysis. Data were analyzed with John's Macintosh Project (JMP) v.8.0 or v.14.1.0 software (SAS Institute, Cary, NC) using one-way ANOVA and a Dunnett's test post hoc. Statistical outliers were identified from the entire dataset using the distribution tool with a boxplot outlier analysis in JMP software with data points greater than 1.5 times the interquartile range being excluded from further statistical analysis. In cases where data appeared skewed, log transformation of the data was done with a Box Cox transformation prior to applying one-way ANOVA and the Dunnett's test. The test *P* values in the results provided are raw and not adjusted for multiple testing.

Results

In Vitro Activity of Peptides. A modified version of human UCN1 with insertion of the frog sauvagine sequence "EKQEKEKQ" from aa 21–28 to reduce binding to CRH binding protein (Isfort et al., 2006) and insertion of a cysteine residue at position 31 for pegylation was generated to provide extended exposure duration in vivo. The amino acid sequence of the PEG-hUCN1 peptide is DNPSLSIDLTFHLLRTLLELE KQEKEKQQA C(PEG20 acetamide)QNRIIFDSV-NH2. The PEG-hUCN1 was tested in vitro for activity in PathHunter eXpress beta arrestin assays at the mouse CRHR1 receptor and the human CRHR2 receptor and compared with native human CRH, UCN1, or UCN2 peptides. At the CRHR1 receptor, the PEG-hUCN1 peptide was less potent than native CRH or UCN1 peptides with EC_{50} values of 47, 15, and 10 nM, respectively (log EC_{50} ± S.E.M. of 1.674 ± 0.011, 1.19 ± 0.04, and 0.992 ± 0.019, respectively). At the CRHR2 receptor, the PEG-hUCN1 peptide was also less potent than UCN2 or UCN1 peptides with EC_{50} values of 80, 10, and 6.6 nM, respectively (log EC_{50} ± S.E.M of 1.895 ± 0.005, 0.984 ± 0.032, and 0.822 ± 0.004, respectively).

TABLE 1
Pharmacokinetic parameters of pegylated hUCN1Pharmacokinetic data from plasma were calculated after a single subcutaneous administration to female C57BL/6J mice (n = 2 per timepoint). PK parameters were calculated using the N-terminal peptide concentrations.

Dose (mg/kg)	C_{max} (ng/ml)	T_{max} (hr)	$AUC_{0\text{-}inf}$ (hr*ng/ml)	$T_{1/2}$ (hr)	CL/F (ml/hr/kg)
0.3	505	8	17479	13	17.2
1	1951	24	68866	17	14.5

$AUC_{0\text{-}inf}$, area under the curve from time 0 to infinity; CL/F, apparent clearance; C_{max}, maximum plasma concentration; $T_{1/2}$, terminal half-life; T_{max}, time of maximum concentrations.

In Vivo Pharmacokinetic and Pharmacodynamic Activity of a Single Dose of PEG-hUCN1. The pharmacokinetics of PEG-hUCN1 were evaluated in mice after a single subcutaneous administration of 0.3 or 1 mg/kg. The time to achieve maximum PEG-hUCN1 plasma concentrations ranged from 8–24 hours. The plasma concentration was roughly proportional to dose. The half-life at 1 mg/kg was 17 hours. Pharmacokinetic data for PEG-hUCN1 are shown in Table 1.

We next determined the pharmacodynamic response of a single injection of PEG-hUCN1 at a dose level of 1 mg/kg by measuring serum corticosterone over 3 days. Corticosterone became elevated with a maximum effect observed at 6 hours and remained elevated above controls out to 72 hours post injection (Fig. 1A). A single dose response study from 0.003 to 1 mg/kg of PEG-hUCN1 demonstrated that the serum corticosterone response at 6 hours post injection was highly sensitive to PEG-hUCN1 and returned to baseline by 96 hours post injection except at 1 mg/kg (Fig. 1B). Measurement of food intake and body weight indicated that at the highest dose level of 1 mg/kg there was reduced food intake and body weight at 24 hours post injection followed by increased food intake and body weight at later timepoints (Fig. 1, C–D). Glucocorticoids are known to promote lymphoid atrophy, and an assessment of spleen and thymus weight at the end of the 96 hours indicated a dose response effect of the PEG-hUCN1 on reducing the weight of these lymphoid tissues (Fig. 1E). Significant reductions in spleen weight were seen at the 0.1 and 0.03 mg/kg dose levels ($P < 0.05$), whereas thymus weight was significantly reduced at all dose levels ($P < 0.05$ at 0.003 and 0.01 mg/kg; $P < 0.001$ at 0.03 mg/kg; and $P < 0.01$ at 1 and 0.1 mg/kg). Thymic cell counts confirmed that reduction of thymus weight was due to a loss of thymic cells in a similar dose response manner ($P < 0.01$ at 0.003 and 0.01 mg/kg; $P < 0.001$ at 0.03, 0.1, and 1 mg/kg) (Fig. 1F).

In Vivo Activity of Multiple Doses of PEG-hUCN1. A multiple dose response study of two injections of PEG-hUCN1 from 0.1–1 mg/kg given 4 days apart was conducted to

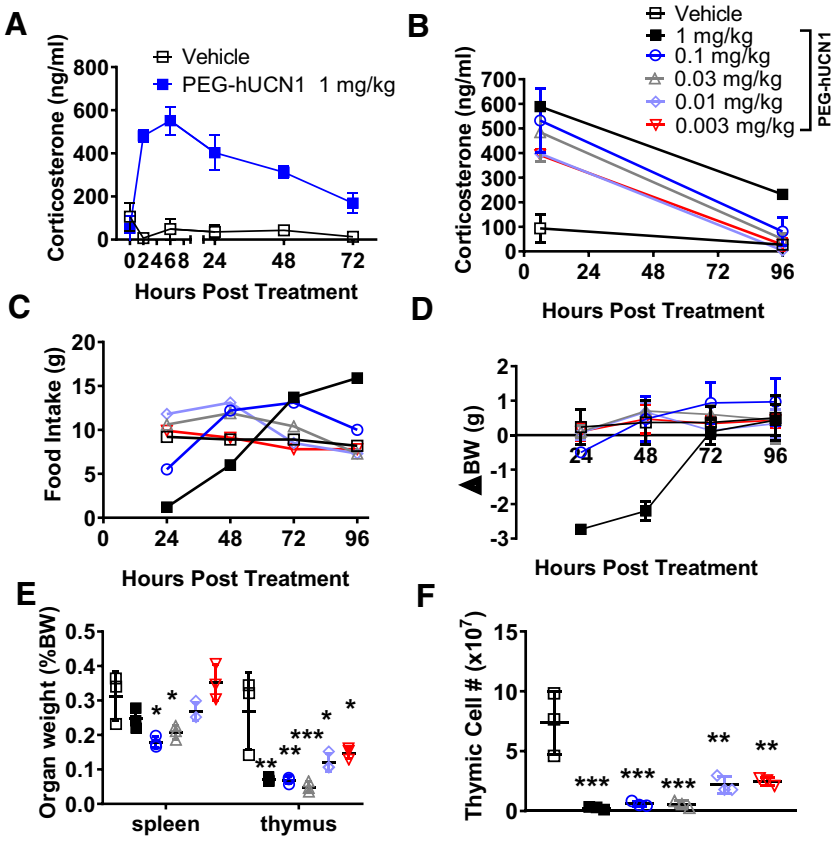

Fig. 1. In vivo activity of PEG-hUCN1 in healthy female C57BL/6J mice at 7–8 weeks of age. (A) In vivo serum corticosterone pharmacodynamic response to a single subcutaneous injection of 1 mg/kg of PEG-hUCN1 over time. (B–F) Single ascending dose response study of PEG-hUCN1 demonstrates dose dependent elevation in serum corticosterone (B) and effects on food intake (C), body weight (D), spleen and thymus weights (E), and thymic cell counts (F). Values shown represent the mean ± S.D. for three subjects except for panel C, which shows total food consumed per three mice at each timepoint. Statistical significance was determined using one-way ANOVA followed by a Dunnett's post-test. $*P < 0.05$, $**P < 0.01$, $***P < 0.001$ relative to the vehicle group.

determine effects on serum corticosterone, food intake, and body weight. Serum corticosterone increased in a dose response manner after the first injection, reached a maximum by 6 hours post injection, and returned to near baseline only at the lowest dose level, whereas the corticosterone response after the second injection was strikingly subdued at the higher dose levels (Fig. 2A). Food intake was reduced during the first 24 hours in a dose dependent manner, and then intake increased by the third and fourth days post injection. Food intake after the second injection was slightly reduced in the first 24 hours, then remained elevated thereafter at all dose levels relative to vehicle, with a return to baseline values by 8 days after the second injection (Fig. 2B). In contrast to increased food intake, body weight showed only small insignificant increases at all dose levels relative to vehicle (Fig. 2C).

We next ran a chronic 4-week study dosing PEG-hUCN1 subcutaneously at 1 mg/kg once weekly and compared this regimen to administering corticosterone to mice in the drinking water to compare effects on the spleen and thymus. Serum corticosterone was elevated by the PEG-hUCN1 out to 4 days post injection but returned to baseline by 7 days, whereas administration of corticosterone in the drinking water remained elevated at all timepoints measured (Fig. 3A). At the end of the 4-week study, similar significant effects on splenic and thymic atrophy ($P < 0.0001$) were observed with both treatments (Fig. 3, B–C).

PEG-hUCN1 Improves Disease Severity and Histology in Imiquimod Induced Skin Inflammation Model. PEG-hUCN1 at a low (0.03 mg/kg s.c.) and a high (1 mg/kg s.c.) dose level, as well as prednisolone [10 mg/kg by mouth (PO) once daily (QD)], were tested in an experimental mouse model of imiquimod induced skin inflammation with treatment administered at days -2 and 3 relative to imiquimod injection. The disease score increased from day 0–7 in the vehicle groups, whereas treatment with prednisolone resulted in significantly improved scores ($P < 0.0001$) beginning at day 4 out to day 7 (Fig. 4A). Comparable to prednisolone, treatment with PEG-hUCN1 at both dose levels resulted in significantly reduced disease scores versus vehicle ($P < 0.0001$). Histopathological scoring of skin at the end of the study demonstrated significant pathology in the vehicle groups relative to naive skin ($P < 0.0001$), whereas the prednisolone and 0.03 mg/kg PEG-hUCN1 treatment groups showed a similar significant improvement in skin histopathology relative to the respective vehicle group ($P < 0.001$) (Fig. 4, B–C).

PEG-hUCN1 Improves Clinical Score and Histology in Established Arthritis CIA Mouse Model. To determine whether therapy with PEG-hUCN1 could improve established arthritic disease in an experimental model of collagen induced arthritis, mice with arthritis were treated with either prednisolone (10 mg/kg PO QD) or two dose levels of PEG-hUCN1 (0.03 and 0.1 mg/kg s.c. q5d) for 2 weeks beginning on day 28. All groups started with an average clinical arthritis score above 3 on a scale from 0–5, and the clinical score in the vehicle groups continued to worsen out to day 42 with an average score near 5 (Fig. 5A). Prednisolone treatment resulted in a rapid resolution of disease score that approached an average score of 0 by day 36. Treatment with PEG-hUCN1 dose dependently reduced the clinical score, with the 0.1 mg/kg dose resulting in an average clinical score of near 1 by day 42. A statistical analysis of the area under the curve for clinical scoring indicated significant improvements in disease with

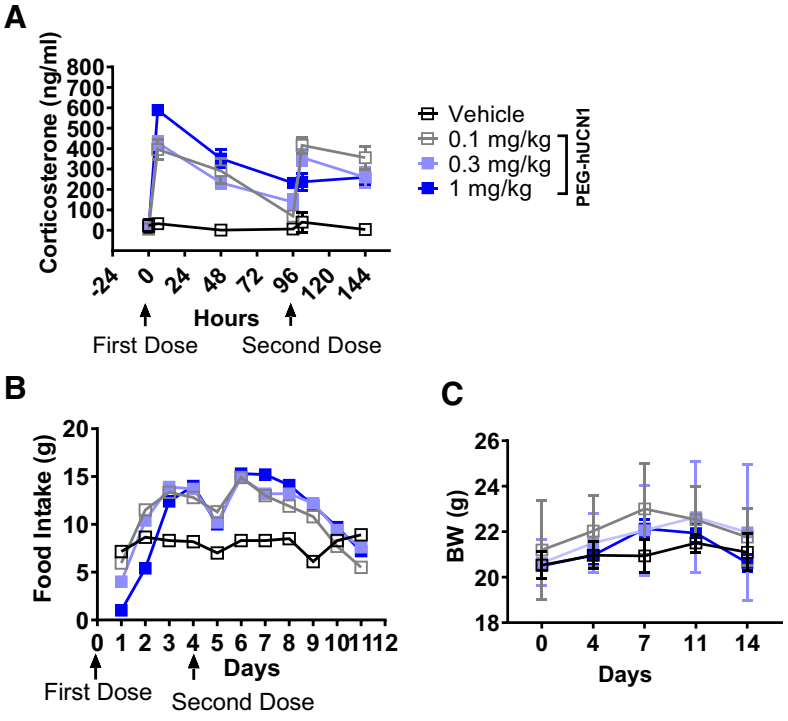

Fig. 2. Multiple ascending dose study of PEG-hUCN1 on in vivo activity in healthy female C57BL/6J mice at 12–13 weeks of age. (A–C) A 2-week study with two doses of PEG-hUCN1 at 0.1, 0.3, or 1 mg/kg administered subcutaneously on days 0 and 4 with measurement of serum corticosterone (A), food intake (B), and body weight (C) at indicated timepoints. Values represent the mean ± S.D. for three subjects except for food intake, which is shown as food consumed for three mice per timepoint.

all treatments versus vehicle ($P < 0.0001$) (Fig. 5A). As shown in Fig. 5B, histologic scoring of paw tissue demonstrated a significant reduction in histopathology scores for the 0.03 mg/kg dose of PEG-hUCN1 ($P < 0.01$) and similar reductions in scores with both prednisolone and the 0.1 mg/kg PEG-hUCN1 treatments relative to the respective vehicle control ($P < 0.0001$). Although spleen weight was increased in the vehicle disease groups relative to the naive control, all treatments resulted in significant reductions in spleen weight with prednisolone and the 0.1 mg/kg dose of PEG-hUCN1 having the greatest effect ($P < 0.0001$ and $P < 0.001$, respectively) (Fig. 5C). Representative images of forepaw histology are shown in Fig. 5D.

PEG-hUCN1 Improves Disease in Experimental Relapsing Remitting EAE. PEG-hUCN1 improved autoimmune disease in experimental models of Psoriasis and Arthritis, so we next tested the molecule in an experimental model of relapsing remitting EAE. The proteolipid protein 139-151 peptide was injected into mice with CFA and pertussis toxin to initiate the disease on day 0 with scoring starting on day 9 and prednisolone (10 mg/kg PO QD) or PEG-hUCN1 (0.03 and 0.1 mg/kg sc q5d) treatment initiated on day 12. Average EAE disease scores were near 1.5 on a scale of 0–5 at the time of treatment initiation, and all treatments resulted in a reduction in disease score that was apparent by day 19, with a significant effect by the end of the study relative to the vehicle control

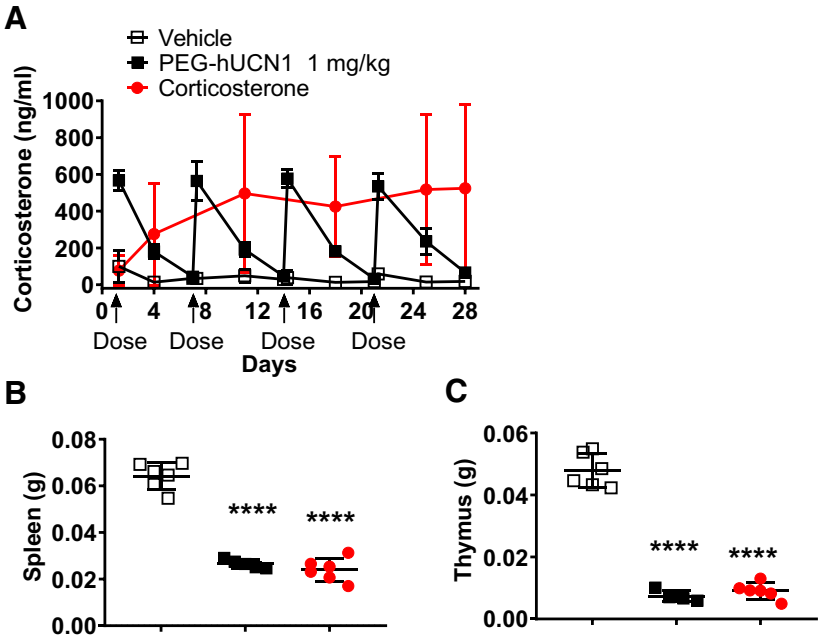

Fig. 3. Comparison of PEG-hUCN1 to corticosterone administered in the drinking water over 4 weeks. Healthy female C57BL/6J mice at 11–12 weeks of age were injected subcutaneously with vehicle or PEG-hUCN1 at 1 mg/kg once weekly or administered corticosterone in the drinking water at 100 mcg/ml. (A) Serum corticosterone at indicated timepoints, (B) spleen, and (C) thymus weights at the end of the study. Data represent the mean ± S.D. for six subjects. Statistical significance was determined using one-way ANOVA followed by a Dunnett's post-test. ****$P < 0.0001$ relative to vehicle group.

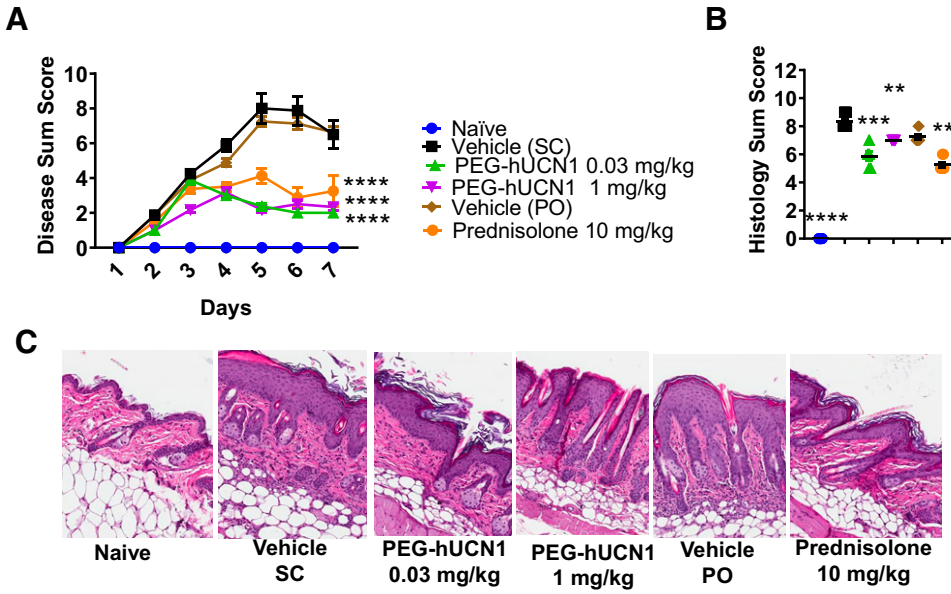

Fig. 4. Effects of PEG-hUCN1 in a murine model of imiquimod induced skin inflammation. A 7-day study with prednisolone given PO once daily at 10 mg/kg beginning on day -2 or vehicle and PEG-hUCN1 (0.03 and 1 mg/kg) treatments given on days -2 and 3, and imiquimod administered on day 1. (A) Clinical disease sum score, (B) histology sum score, and (C) representative histology sections are shown for the naïve, vehicle (subcutaneously), 0.03 and 1 mg/kg PEG-hUCN1, HEC vehicle (PO), and prednisolone groups. H&E stain (10X) for histology sections. Values for eight subjects per group represent the mean ± S.D. except in panel A with mean ± S.E.M. Statistical significance was determined using one-way ANOVA followed by a Dunnett's post-test. $^{**}P < 0.01$, $^{***}P < 0.001$, $^{****}P < 0.0001$ versus respective vehicle.

($P < 0.001$ for the PEG-hUCN1 groups and $P < 0.01$ for the prednisolone group) (Fig. 6A). A statistical analysis of the area under the curve for disease scoring indicated that only the 0.1 mg/kg PEG-hUCN1 treatment significantly reduced EAE score ($P < 0.05$) (Fig. 6B). Histopathological scoring of spinal cord indicated that although both the 0.03 and 0.1 mg/kg PEG-UCN1 treatments significantly improved demyelination scores ($P < 0.01$) (Fig. 6C), only the 0.1 mg/kg PEG-hUCN1 treatment significantly improved inflammatory scores ($P < 0.05$) (Fig. 6D) and apoptotic cell scores ($P < 0.05$) (Fig. 6E).

Effects of PEG-hUCN1 in the MRL lpr Mouse Model of Lupus. To assess the ability of PEG-hUCN1 to improve autoimmune lupus, we next tested the molecule at a dose level of 0.1 mg/kg (s.c. q4d) over 2 weeks in the MRL lpr model. Measurements of serum corticosterone indicated that PEG-hUCN1 dosing significantly increased serum corticosterone to around 300 ng/ml (~1 micromolar) at 6 hours post dose that returned to near baseline values at 96 hours (Fig. 7A). Spleen weight and serum globulins were significantly elevated with disease relative to the MRL nondisease

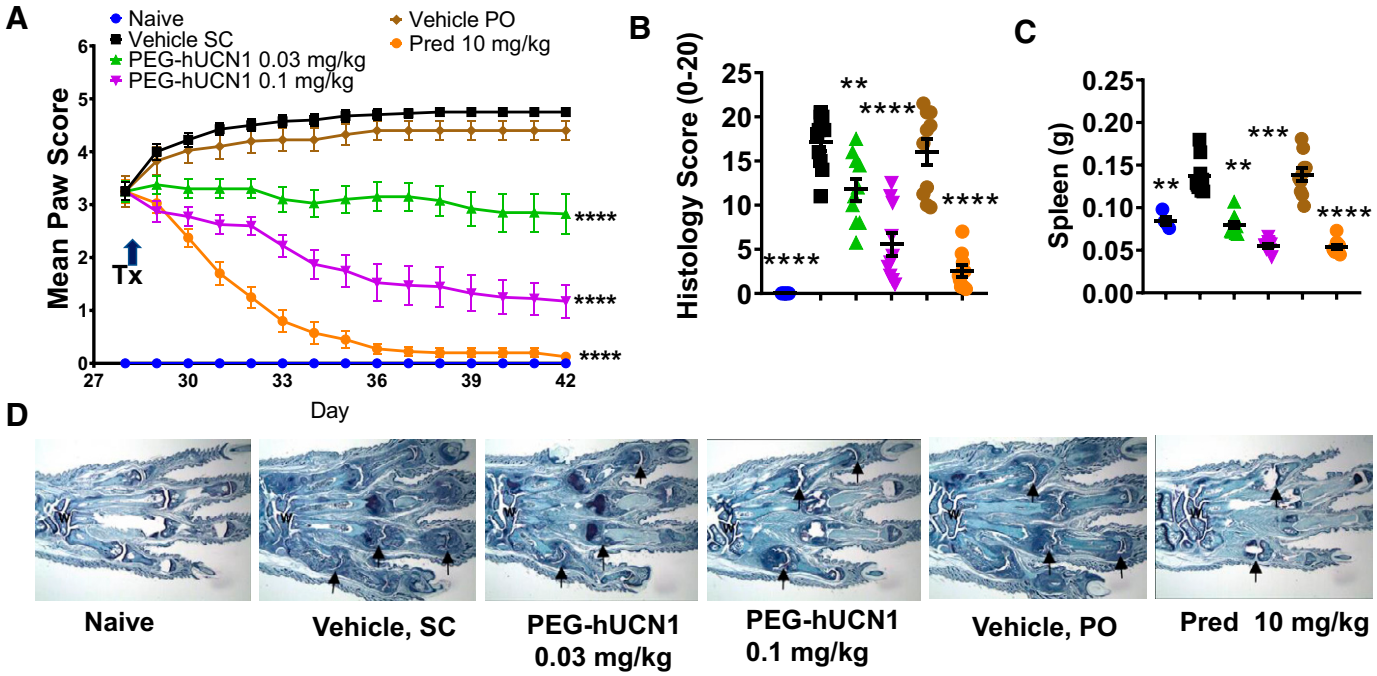

Fig. 5. PEG-hUCN1 treatment in a murine experimental collagen induced arthritis model. A 42-day study with immunization emulsion administered on days 0 and 21, treatment initiation on day 28, and necropsy on day 42. The clinical arthritis paw score over time (A), histology sum score (B), spleen weight (C), and forepaw histology (D) are shown for the naïve, vehicle (s.c. q5d), PEG-hUCN1 (0.03 and 0.1 mg/kg s.c. q5d), HEC vehicle (PO QD), and prednisolone (Pred 10 mg/kg PO QD) groups. Toluidine blue stain (10X) for histology sections showing representative forepaw images for the respective groups with inflammation, cartilage damage, pannus, bone resorption, and periosteal bone formation in the vehicle treated mouse, whereas PEG-hUCN1 and Prednisolone treatment improved the disease severity. Arrows identify representative affected joints. Data are shown as the mean ± S.D. except in panel A with mean ± S.E.M. ($n = 10$ per group except naïve with $n = 4$ per group). Statistical significance was determined using one-way ANOVA followed by a Dunnett's post-test. $^{**}P < 0.01$, $^{***}P < 0.001$, $^{****}P < 0.0001$ versus the respective vehicle control.

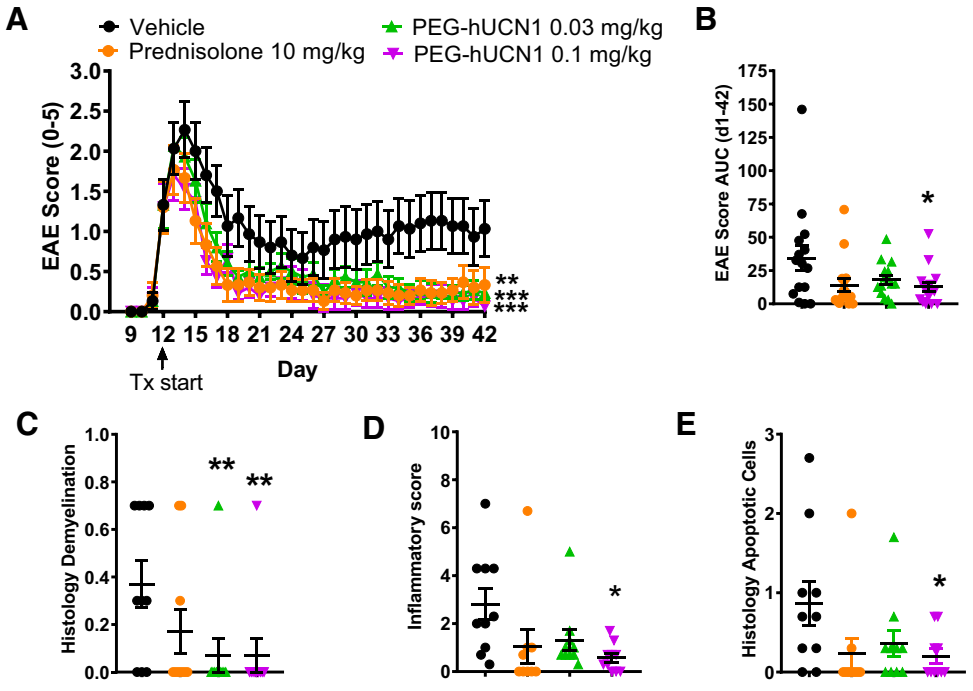

Fig. 6. Effects of PEG-hUCN1 on disease severity in an experimental EAE model. A 42-day study with proteolipid protein (PLP) 139-151 peptide in CFA and pertussis toxin (PTX) administered on day 0, scoring initiated on day 9, treatment initiation on day 12, and necropsy on day 42. Scores are shown for clinical EAE over time (A), EAE area under the curve (AUC) d1-42 (B), histology inflammatory (C), histology demyelination (D), and histology apoptotic cells (E) for the vehicle (s.c. q5d), prednisolone PO (Pred 10 mg/kg QD), and PEG-hUCN1 (0.03 and 0.1 mg/kg q5d) groups. Values represent the mean ± S.D. except in panel A with mean ± S.E.M. N equals 15 subjects per group. Statistical significance was determined using one-way ANOVA followed by a Dunnett's post-test. $^{*}P < 0.05$, $^{**}P < 0.01$, $^{***}P < 0.001$ versus vehicle.

group ($P < 0.0001$) and were significantly reduced with PEG-hUCN1 treatment versus vehicle ($P < 0.001$ and $P < 0.05$, respectively) (Fig. 7, B and C). Although urine albumin to creatinine ratio ($P < 0.0001$), serum blood urea nitrogen ($P < 0.05$), and creatinine ($P < 0.05$) were all significantly elevated in the disease control group relative to the nondisease group, treatment with PEG-hUCN1 significantly reduced serum creatinine relative to the vehicle group ($P < 0.05$) with an insignificant reduction in serum blood urea nitrogen and albumin/creatinine ratio (Fig. 7, D–F).

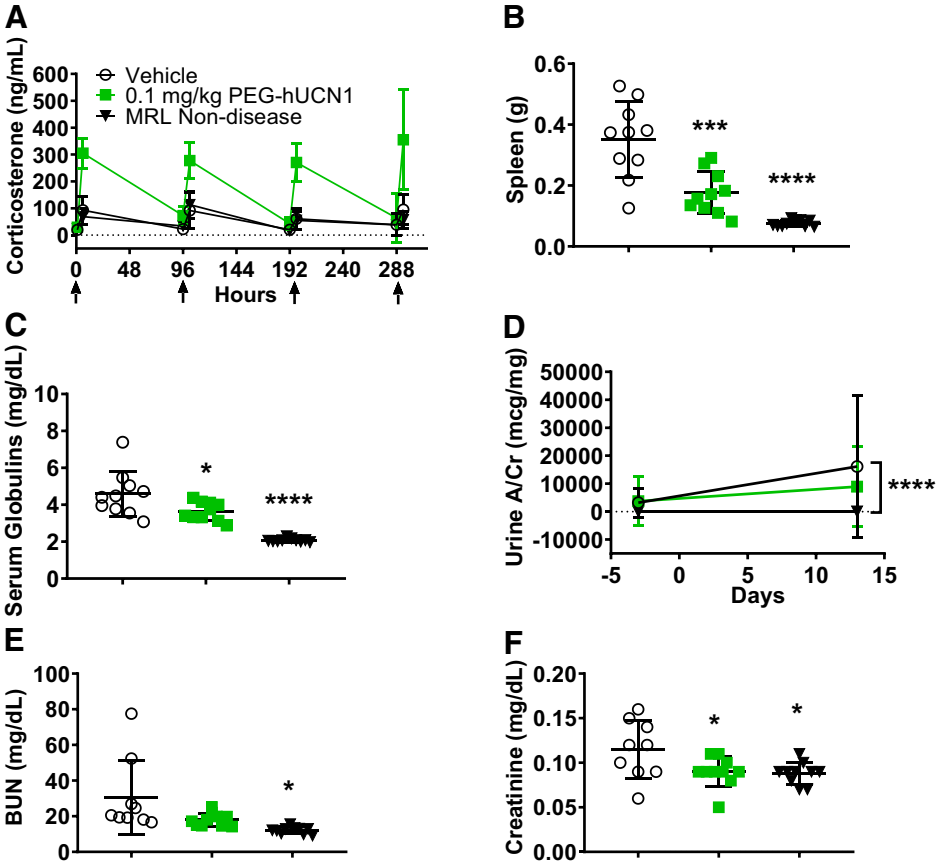

Fig. 7. Effects of PEG-hUCN1 on disease in the MRL lpr model of lupus. MRL lpr mice were aged out to 14 weeks with doses of 0.1 mg/kg PEG-hUCN1 administered s.c. q4d over 2 weeks. Untreated MRL wt (non-disease) mice were used as controls. (A) Serum corticosterone measured 6 hours post dose (dosing indicated by arrows). Effects of PEG-hUCN1 therapy on spleen weight (B), serum globulins (C), urine albumin to creatinine ratio (A/Cr) (D), serum blood urea nitrogen (E), and serum creatinine (F) are shown. Values represent the mean ± S.D. for 9–10 subjects. Urine A/Cr data were log transformed by Box Cox transformation prior to application of statistical analysis. Statistical significance was determined using one-way ANOVA followed by a Dunnett's post-test. $^{*}P < 0.05$, $^{***}P < 0.001$, $^{****}P < 0.0001$ versus vehicle.

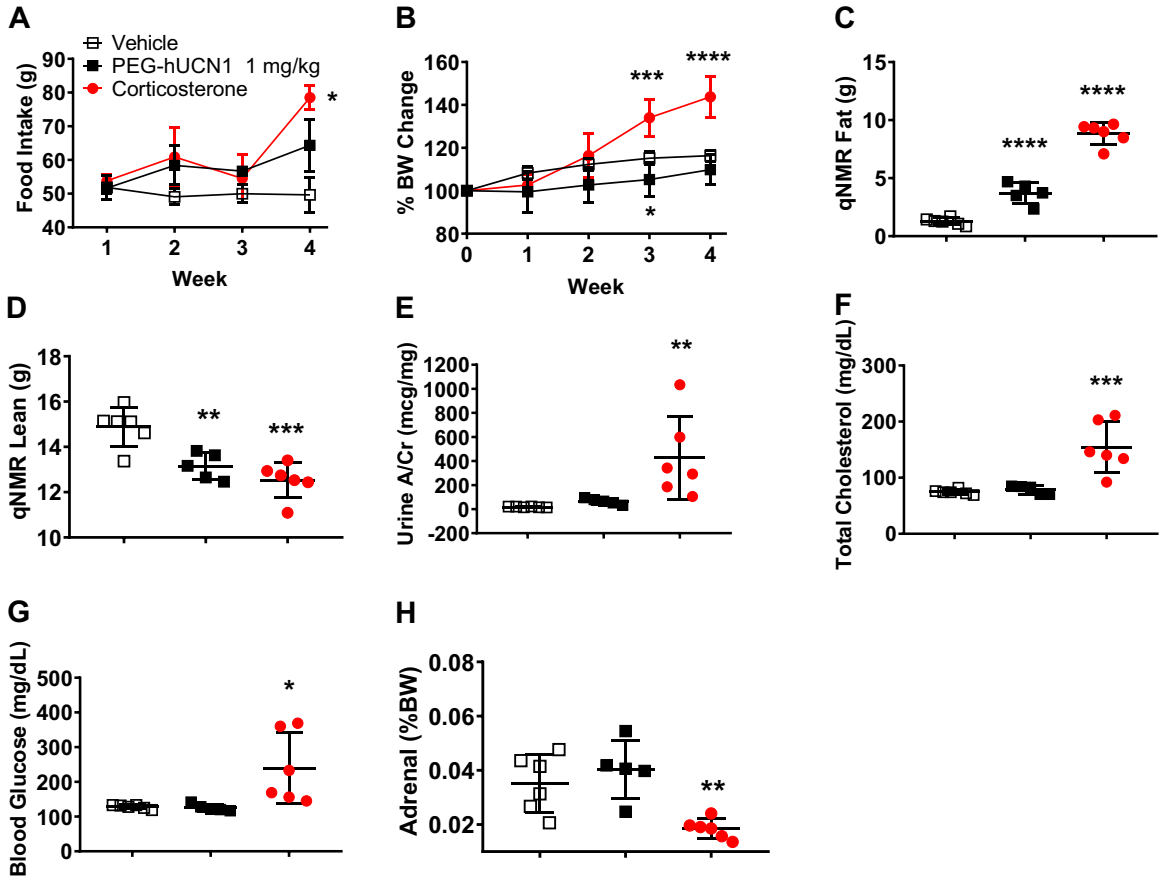

Fig. 8. Effects of PEG-hUCN1 on adverse metabolic effects relative to corticosterone administration in healthy female C57BL/6J mice at 11–12 weeks of age. Corticosterone was administered in the drinking water at 100 mcg/ml, whereas PEG-hUCN1 (1 mg/kg) or vehicle was dosed subcutaneously once weekly, and various parameters were measured. Effects on food intake (A) and body weight (B) are shown over the course of the 4-week study. The effects of corticosterone and PEG-hUCN1 treatment on qNMR fat mass (C), qNMR lean mass (D), urine A/Cr (E), serum total cholesterol (F), fed blood glucose (G), and adrenal gland weight as a percentage of body weight (H) taken at the end of the study are shown. Values represent the mean ± S.D. for six subjects. Statistical significance was determined using one-way ANOVA followed by a Dunnett's post-test. *$P < 0.05$, **$P < 0.01$, ***$P < 0.001$, ****$P < 0.0001$ versus vehicle.

PEG-hUCN1 Shows Improved Metabolic Profile Compared with Corticosterone. Chronic glucocorticoid therapy results in adverse metabolic effects, so we compared once weekly PEG-hUCN1 at 1 mg/kg to administration of corticosterone in the drinking water (100 mcg/ml) over 4 weeks on metabolic parameters in healthy C57BL/6J mice. Both treatments resulted in elevations in serum corticosterone levels over 4 weeks that resulted in equivalent significant reductions in spleen and thymus weights relative to controls, as shown previously in Fig. 3A. Only corticosterone treatment resulted in significantly increased food intake ($P < 0.05$) and body weight ($P < 0.0001$) over the 4 weeks relative to the vehicle control (Fig. 8, A–B), whereas the PEG-hUCN1 treatment showed a significant reduction in body weight at week 3 ($P < 0.05$) (Fig. 8B). Measurement of fat and lean mass by qNMR after 4 weeks demonstrated that corticosterone treatment significantly increased fat mass ($P < 0.0001$) and reduced lean mass ($P < 0.001$) relative to the vehicle group, whereas treatment with PEG-hUCN1 resulted in a similarly significant but lesser effect on fat mass ($P < 0.0001$) and lean mass ($P < 0.01$) (Fig. 8, C–D). Only corticosterone treatment significantly increased the urine albumin to creatinine ratio relative to the vehicle group ($P < 0.01$) (Fig. 8E). Corticosterone administration for 4 weeks also significantly increased serum total Cholesterol ($P < 0.001$) and fed blood glucose ($P < 0.05$) while significantly reducing adrenal gland mass as a percent of body weight ($P < 0.01$) relative to the vehicle group, which was not seen with PEG-hUCN1 treatment (Fig. 8, F–H).

PEG-hUCN1 Has Effects on Blood Pressure and Heart Rate. As native UCN1 has known cardiovascular effects, we next conducted a cardiovascular assessment of a single dose of PEG-hUCN1 at 0.3 and 1 mg/kg in mice implanted with telemetry devices for continuous monitoring of heart rate and blood pressure over 96 hours and compared with dosing with the native UCN1 peptide at 0.1 mg/kg. All mice on study were initially dosed with vehicle and showed an initial rapid increase in blood pressure and heart rate that returned to normal values within an hour. Blood pressure ranged from 75–110 mm Hg (Supplemental Fig. 1A) and heart rate from 500–675 beats per minute (Supplemental Fig. 2A) over the 24-hour diurnal cycle, with increases observed for both measurements during the dark phase. Mice dosed with native UCN1 and the higher dose of PEG-hUCN1 showed an abrupt and striking reduction in blood pressure (nearly 40 mm Hg) relative to baseline that recovered back to the normal diurnal range by 6 hours and then remained elevated in all the groups during the

ensuing light phase (Supplemental Fig. 1B). Although blood pressure in the native UCN1 group returned to a normal diurnal rhythm by 42 hours post dose, both PEG-hUCN1 groups remained elevated with the lower dose, returning to a normal rhythm by 72 hours and the higher dose still elevated at 96 hours (Supplemental Fig. 1C). In comparison with vehicle dosing, heart rate slightly increased within all groups in the first 12 hours followed by a dramatic reduction in heart rate out to 24 hours in the native UCN1 and 1 mg/kg PEG-hUCN1 groups (Supplemental Fig. 2B). Heart rate recovered to a normal diurnal rhythm in all groups by 30 hours post dose and remained so out to 96 hours (Supplemental Fig. 2C).

Chronic Elevation of UCN1 by AAV8 Delivery Results in Dose Dependent Adverse Metabolic Effects. Since weekly dosing with PEG-hUCN1 at 1 mg/kg did not elevate serum corticosterone over the entire weekly period due to the pharmacokinetic properties of the molecule (see Fig. 3A and Table 1), and to avoid daily dosing, we decided to take an AAV approach to maintain increased circulating mouse UCN1 levels chronically to determine effects on metabolic parameters. A 2-week dose response study was conducted with an AAV8 mouse UCN1 at 10^9, 10^{10}, 10^{11}, and 5×10^{11} gcu per mouse. There was a dose dependent increase in body weight that was significant for the 10^{11} and 5×10^{11} dose levels relative to the AAV8 null ($P < 0.05$ and $P < 0.01$, respectively) (Supplemental Fig. 3A). Serum fed glucose at the end of 2 weeks was significantly elevated in the three highest dose groups relative to the AAV8 null ($P < 0.01$ for the 5×10^{11} group and $P < 0.001$ for the 10^{11} and 10^{10} groups), whereas serum total cholesterol was significantly elevated in the two highest dose groups relative to the AAV8 null ($P < 0.0001$) (Supplemental Fig. 3, B–C). Thymus weights as a % of body weight were significantly increased at the two lowest doses of AAV8 UCN1 relative to the AAV8 null group ($P < 0.05$ for the 10^9 group and $P < 0.01$ for the 10^{10} group) and were significantly decreased at the two highest dose levels ($P < 0.05$) (Supplemental Fig. 3D). Spleen weight as a % of body weight was significantly increased relative to the AAV8 null at the lowest dose level of AAV8 UCN1 ($P < 0.05$) and was significantly decreased at the two highest dose levels ($P < 0.01$).

Effects of AAV8 UCN1 Compared with Corticosterone on Adipose, Muscle, and Bone. Glucocorticoids have profound effects on adipose, skeletal muscle, and bone; thus, we examined the effects of AAV8 UCN1 at 10^{11} gcu/mouse versus corticosterone administered in the drinking water at 100 mcg/ml to healthy female C57BL/6J mice. As shown in Supplemental Fig. 4, A–B, both corticosterone and AAV8 UCN1 induced similar increases in adipose tissue by qNMR method ($P < 0.0001$) and measurement of gonadal fat pad mass ($P < 0.01$) relative to AAV8 null mice. Both treatments also induced similarly significant losses in muscle mass as measured by qNMR method ($P < 0.0001$) and measurement of quadriceps muscle mass ($P < 0.0001$) relative to the AAV8 null group (Supplemental Fig. 4, C–D). However, although corticosterone induced a slight decrease in distal femur bone mineral density (BMD) and a significant decrease in midfemur BMD ($P < 0.01$) relative to the AAV8 null group, AAV8 UCN1 administration resulted in a significant increase in distal BMD ($P < 0.001$) and no effect on midfemur BMD (Supplemental Fig. 4, E–F).

Adverse Effects of AAV8 UCN1 in CRHR2 Knockout Mice. Since UCN1 can signal through CRHR1 to elevate corticosterone and through CRHR2 to promote beneficial metabolic effects, we evaluated the effects of an AAV8 null or AAV8 UCN1 in CRHR2 knockout mice (KO) and wild type (WT) littermates to determine the contribution of the CRHR2 receptor to the observed metabolic effects. CRHR2 KO mice consumed significantly more food ($P < 0.05$) and had significantly greater body weight ($P < 0.0001$) relative to WT mice (Supplemental Fig. 5, A–B). Administration of AAV8 UCN1 significantly increased food intake only in CRHR2 KO mice ($P < 0.01$) relative to the respective AAV8 null group (Supplemental Fig. 5A). Increased food intake led to a significant increase in body weight only in the AAV8 UCN1 CRHR2 KO group ($P < 0.01$) (Supplemental Fig. 5B). Fasted blood glucose taken at the end of the study was similar in CRHR2 KO mice relative to WT mice, and administration of AAV8 UCN1 significantly increased fasted blood glucose only in the CRHR2 KO group ($P < 0.0001$) relative to the AAV8 null KO group (Supplemental Fig. 5C). Total cholesterol in serum was significantly lower in CRHR2 KO mice relative to WT mice ($P < 0.01$), and administration of AAV8 UCN1 significantly increased total cholesterol only in the CRHR2 KO group ($P < 0.0001$) (Supplemental Fig. 5D). Fat mass measured by qNMR as a % of body weight was significantly greater at week 4 in CRHR2 KO mice compared with WT mice ($P < 0.01$), whereas lean mass was not different (Supplemental Fig. 5, E–F). Administration of AAV8 UCN1 significantly increased fat mass ($P < 0.0001$) and significantly decreased lean mass ($P < 0.0001$) only in CRHR2 KO mice relative to the respective AAV8 null group (Supplemental Fig. 5, E–F). Urine albumin to creatinine ratio was significantly increased only in the CRHR2 KO group given AAV8 UCN1 relative to the KO control group ($P < 0.001$) (Supplemental Fig. 5G). CRHR2 KO mice showed significantly reduced adrenal gland mass as a % of body weight relative to WT mice ($P < 0.05$), and administration of AAV8 UCN1 resulted in a significantly further reduction in adrenal gland mass in the CRHR2 KO group relative to the control AAV8 KO group ($P < 0.01$) (Supplemental Fig. 5H).

Discussion

The CRH family of peptides have notably short half-lives in humans with a half-life of 52 minutes for UCN1 (Davis et al., 2004). The major purpose of this study was to generate a long acting pegylated UCN1 peptide and an AAV8 UCN1 to extend the exposure duration of the peptide to determine efficacy in autoimmune disease models, as well as establish a safety profile of adverse effects. The main findings of the study demonstrated equivalent effects of the peptide in several autoimmune disease models relative to prednisolone with an improved safety profile over orally administered corticosterone in healthy animals that was dependent on the presence of the CRHR2 receptor. Pegylation of the UCN1 peptide reduced in vitro activities at the CRH receptors while providing prolonged exposure in vivo with a half-life of 13–17 hours, depending on the dose level. To our knowledge, there are no known studies testing a long acting UCN1 peptide in experimental autoimmune disease or examining adverse metabolic effects from such an experimental therapy in comparison with glucocorticoids. Although native UCN1 peptide has been shown to improve autoimmune disease in murine experimental colitis

and rheumatoid arthritis with demonstrated effects on Th1/Th17/Treg related cytokines (Gonzalez-Rey et al., 2006a, 2007), the dependence of these effects on endogenous production of corticosterone was not evaluated, nor was a comparison with glucocorticoid therapy included. In our study, we have demonstrated a pharmacodynamic corticosterone response to PEG-hUCN1 with maximal induction of serum corticosterone to around 600 ng/ml (~2 micromolar) at 1 mg/kg. For comparison, a 1 microgram dose (~0.04 mg/kg) of native UCN1 given subcutaneously to mice increased corticosterone levels to around 150 ng/ml (~0.5 micromolar) (Agnello et al., 1998). In addition, we have compared the therapeutic benefit of our pegylated UCN1 in several autoimmune models to the widely used clinical drug prednisolone. The efficacy obtained in our autoimmune models was similar between PEG-hUCN1, and steroid therapy and the endogenous corticosterone levels from PEG-hUCN1 administration reached levels in blood $\geq$ 1 micromolar. The levels of corticosterone in that range have been shown to have potent anti-inflammatory and antiproliferative effects on immune cells (Sandi et al., 1992; Liao et al., 1995); thus, we speculate that mechanistically the observed benefits in our experimental models from PEG-hUCN1 are mainly due to elevated corticosterone levels and the direct effects of this glucocorticoid on immune cells. For a review on mechanisms of glucocorticoids on immune cells, see Rhen and Cidlowski (2005). The expression of CRHR1 and CRHR2 receptors has been reported in immune cells; thus, we cannot rule out a direct effect of PEG-hUCN1 on immune cells in the responses we observed. Although the CRH family of peptides have shown both pro- and anti-inflammatory effects on immune cells (Gravanis and Margioris, 2005), a more detailed characterization of the direct effects of these peptides on immune cells is warranted to better understand their role in immune responses independent of glucocorticoids.

Although the administration of PEG-hUCN1 was predicted to improve autoimmune disease in animal models due to endogenous corticosterone production, the effects of such a therapy on adverse effects due to UCN1 induced glucocorticoids have not been studied previously, but would be relevant clinically. The observed effects of PEG-hUCN1 on acute reductions in food intake and body weight agree with published observations of UCN peptides that activate the CRHR2 receptor (Asakawa et al., 1999). The subsequent increase in food intake that was observed with longer exposure to the long acting peptide could be attributed to elevations in endogenous corticosterone. Glucocorticoids are known to stimulate appetite and are believed to do so through actions in the hypothalamus (Bruce et al., 1982; King, 1988). Other observed adverse effects seen with the PEG-hUCN1 peptide or AAV8 UCN1, such as increases in fat mass, dyslipidemia, and blood glucose and decreases in muscle and adrenal gland mass have been previously attributed to elevated glucocorticoid activity (Wetzels et al., 1988; Berris et al., 2007; Prete and Bancos, 2021; Yasir et al., 2021). Glucocorticoid-induced osteoporosis in patients that receive synthetic glucocorticoids chronically show increased risk of fractures associated with poor quality of life (Ilias et al., 2022). Although corticosterone administration reduced midfemur BMD, we saw no such effect with AAV8 UCN1, and additionally we observed an increase in distal femur BMD. Beneficial effects of UCN1 treatment on femoral trabecular architecture in ovariectomized rats have been previously noted, especially at the distal femur (Tezval et al., 2015). Many of the adverse effects seen with corticosterone administered in the drinking water were notably greater compared with PEG-hUCN1 administration, although we can't rule out that the differences observed were due to different degrees of exposure of the treatments associated with the different dosing paradigms that were used. We speculate that the improved adverse metabolic effects of PEG-hUCN1 are due to CRHR2 activation. UCN peptides that selectively activate the CRHR2 receptor have been shown in previous reports to reduce food intake, body weight, liver triglycerides, and blood glucose, as well as increase skeletal muscle mass and improve insulin sensitivity (Inoue et al., 2003; Isfort et al., 2006; Gao et al., 2016; Kim et al., 2019; Borg et al., 2021). The beneficial metabolic effects of UCN2, a selective CRHR2 peptide, by an AAV approach in high fat diet fed mice were not observed in CRHR2 KO mice (Gao et al., 2016). In our study, we noted that although AAV8 UCN1 induced adverse metabolic effects in C57BL/6J mice, the adverse effects were much less on the WT B6:129 background and exacerbated in the CRHR2 KO mice, suggesting that the background strain is important for metabolic effects, and the CRHR2 receptor plays an important role in countering the adverse metabolic effects induced by endogenous corticosterone. Even without AAV8 UCN1 administration, CRHR2 KO mice exhibited some adverse metabolic effects relative to WT B6:129 mice, suggesting a role for this receptor in metabolism under normal homeostatic conditions.

The cardiovascular profile of the PEG-hUCN1 peptide agrees with the published observations of acute UCN1 administration to rodents with reductions in blood pressure and increases in heart rate that are due to CRHR2 activation (Torpy et al., 1999; Coste et al., 2000). The more chronic effects on the cardiovascular profile observed with sustained exposure to the PEG-hUCN1 peptide in our study with increases in blood pressure and reductions in heart rate have not been reported previously with the native UCN1 peptide in a healthy species. These chronic effects on blood pressure and heart rate over time could be attributed to an elevation in endogenous corticosterone levels resulting from chronic CRHR1 activation in the anterior pituitary. Chronic glucocorticoid exposure is known to increase blood pressure in many species, including humans, although the exact mechanism for this is not clear (Goodwin and Geller, 2012).

In conclusion, we have generated a long acting UCN1 peptide with a prolonged pharmacokinetic profile that exhibits beneficial effects in several murine autoimmune disease models and shows an improved metabolic profile relative to corticosterone that is dependent on CRHR2 activity. These data support the use of UCN1 as a potential therapy for autoimmune diseases. However, potential adverse effects from prolonged elevations in endogenous corticosterone could pose a risk in clinical application.

Authorship Contributions

Participated in research design: Heuer, Meyer, Baker, Martin, Thirunavukkarasu, Alsina-Fernadez, Ma.

Conducted experiments: Meyer, Baker, Geiser, Lucchesi, Xu, Hamang, Hu, Roth.

Contributed new reagents or analytic tools: Geiser, Roth.

Performed data analysis: Heuer, Meyer, Baker, Geiser, Lucchesi, Xu, Hamang, Martin, Hu, Ma.

Wrote or contributed to the writing of the manuscript: Heuer, Meyer, Martin, Roth, Thirunavukkarasu, Alsina-Fernandez, Ma.

Acknowledgments

The authors would like to thank Dr. Wei Ni and Dr. Maria D. Garcia-Castillo for critical reading of the manuscript. The authors would like to thank Jill M. Schroeder for assistance with measurement of serum and urine analytes and Keaton Fiechter, who helped with the LC-MS/MS analysis. The authors would also like to thank Garrett Brickens and Isaiah Clark for assistance with animal studies.

References

Agnello D, Bertini R, Sacco S, Meazza C, Villa P, and Ghezzi P (1998) Corticosteroid-independent inhibition of tumor necrosis factor production by the neuropeptide urocortin. *Am J Physiol* **275**:E757–E762.

Asakawa A, Inui A, Ueno N, Makino S, Fujino MA, and Kasuga M (1999) Urocortin reduces food intake and gastric emptying in lean and ob/ob obese mice. *Gastroenterology* **116**:1287–1292.

Berris KK, Repp AL, and Kleerekoper M (2007) Glucocorticoid-induced osteoporosis. *Curr Opin Endocrinol Diabetes Obes* **14**:446–450.

Borg ML, Massart J, Schönke M, De Castro Barbosa T, Guo L, Wade M, Alsina-Fernandez J, Miles R, Ryan A, Bauer S, et al. (2019) Modified UCN2 peptide acts as an insulin sensitizer in skeletal muscle of obese mice. *Diabetes* **68**:1403–1414.

Borg ML, Massart J, De Castro Barbosa T, Archilla-Ortega A, Smith JAB, Lanner JT, Alsina-Fernandez J, Yaden B, Culver AE, Karlsson HKR, et al. (2021) Modified UCN2 peptide treatment improves skeletal muscle mass and function in mouse models of obesity-induced insulin resistance. *J Cachexia Sarcopenia Muscle* **12**:1232–1248.

Bruce BK, King BM, Phelps GR, and Veitia MC (1982) Effects of adrenalectomy and corticosterone administration on hypothalamic obesity in rats. *Am J Physiol* **243**:E152–E157.

Coste SC, Kesterson RA, Heldwein KA, Stevens SL, Heard AD, Hollis JH, Murray SE, Hill JK, Pantely GA, Hohimer AR, et al. (2000) Abnormal adaptations to stress and impaired cardiovascular function in mice lacking corticotropin-releasing hormone receptor-2. *Nat Genet* **24**:403–409.

Davis ME, Pemberton CJ, Yandle TG, Lainchbury JG, Rademaker MT, Nicholls MG, Frampton CM, and Richards AM (2004) Urocortin-1 infusion in normal humans. *J Clin Endocrinol Metab* **89**:1402–1409.

Dermitzaki E, Venihaki M, Tsatsanis C, Gravanis A, Avgoustinaki PD, Liapakis G, and Margioris AN (2018) The multi-faceted profile of corticotropin-releasing factor (CRF) family of neuropeptides and of their receptors on the paracrine/local regulation of the inflammatory response. *Curr Mol Pharmacol* **11**:39–50.

Gasparini SJ, Weber MC, Henneicke H, Kim S, Zhou H, and Seibel MJ (2016) Continuous corticosterone delivery via the drinking water or pellet implantation: a comparative study in mice. *Steroids* **116**:76–82.

Gao MH, Giamouridis D, Lai NC, Walenta E, Paschoal VA, Kim YC, Miyanohara A, Guo T, Liao M, Liu L, et al. (2016) One-time injection of AAV8 encoding urocortin 2 provides long-term resolution of insulin resistance. *JCI Insight* **1**:e88322.

Gonzalez-Rey E, Fernandez-Martin A, Chorny A, and Delgado M (2006a) Therapeutic effect of urocortin and adrenomedullin in a murine model of Crohn's disease. *Gut* **55**:824–832.

Gonzalez-Rey E, Chorny A, Varela N, Robledo G, and Delgado M (2006b) Urocortin and adrenomedullin prevent lethal endotoxemia by down-regulating the inflammatory response. *Am J Pathol* **168**:1921–1930.

Gonzalez-Rey E, Chorny A, Varela N, O'Valle F, and Delgado M (2007) Therapeutic effect of urocortin on collagen-induced arthritis by down-regulation of inflammatory and Th1 responses and induction of regulatory T cells. *Arthritis Rheum* **56**:531–543.

Goodwin JE and Geller DS (2012) Glucocorticoid-induced hypertension. *Pediatr Nephrol* **27**:1059–1066.

Grammatopoulos DK and Ourailidou S (2017) CRH receptor signalling: potential roles in pathophysiology. *Curr Mol Pharmacol* **10**:296–310.

Gravanis A and Margioris AN (2005) The corticotropin-releasing factor (CRF) family of neuropeptides in inflammation: potential therapeutic applications. *Curr Med Chem* **12**:1503–1512.

Harlé G, Kaminski S, Dubayle D, Frippiat JP, and Ropars A (2018) Murine splenic B cells express corticotropin-releasing hormone receptor 2 that affect their viability during a stress response. *Sci Rep* **8**:143.

Hashimoto K, Nishiyama M, Tanaka Y, Noguchi T, Asaba K, Hossein PN, Nishioka T, and Makino S (2004) Urocortins and corticotropin releasing factor type 2 receptors in the hypothalamus and the cardiovascular system. *Peptides* **25**:1711–1721.

Ilias I, Milionis C, and Zoumakis, E (2022) *An Overview of Glucocorticoid-Induced Osteoporosis*. In: K.R. Feingold, et al. (Eds.), Endotext, South Dartmouth, MA.

Inoue K, Valdez GR, Reyes TM, Reinhardt LE, Tabarin A, Rivier J, Vale WW, Sawchenko PE, Koob GF, and Zorrilla EP (2003) Human urocortin II, a selective agonist for the type 2 corticotropin-releasing factor receptor, decreases feeding and drinking in the rat. *J Pharmacol Exp Ther* **305**:385–393.

Isfort RJ, Wang F, Tscheiner M, Dolan E, Bauer MB, Lefever F, Reichart D, Wehmeyer KR, Reilman RA, Keck BD, et al. (2006) Modifications of the human urocortin 2 peptide that improve pharmacological properties. *Peptides* **27**:1806–1813.

Jamieson PM, Cleasby ME, Kuperman Y, Morton NM, Kelly PA, Brownstein DG, Mustard KJ, Vaughan JM, Carter RN, Hahn CN, et al. (2011) Urocortin 3 transgenic mice exhibit a metabolically favourable phenotype resisting obesity and hyperglycaemia on a high-fat diet. *Diabetologia* **54**:2392–2403.

Kim YC, Truax AD, Giamouridis D, Lai NC, Guo T, Hammond HK, and Gao MH (2019) Significant alteration of liver metabolites by AAV8.Urocortin 2 gene transfer in mice with insulin resistance. *PLoS One* **14**:e0224428.

King BM (1988) Glucocorticoids and hypothalamic obesity. *Neurosci Biobehav Rev* **12**:29–37.

Liao J, Keiser JA, Scales WE, Kunkel SL, and Kluger MJ (1995) Role of corticosterone in TNF and IL-6 production in isolated perfused rat liver. *Am J Physiol* **268**:R699–R706.

Lovenberg TW, Chalmers DT, Liu C, and De Souza EB (1995) CRF2 alpha and CRF2 beta receptor mRNAs are differentially distributed between the rat central nervous system and peripheral tissues. *Endocrinology* **136**:4139–4142.

Papadimitriou A and Priftis KN (2009) Regulation of the hypothalamic-pituitary-adrenal axis. *Neuroimmunomodulation* **16**:265–271.

Patel K, Rademaker MT, Kirkpatrick CM, Charles CJ, Fisher S, Yandle TG, and Richards AM (2012) Comparative pharmacokinetics and pharmacodynamics of urocortins 1, 2 and 3 in healthy sheep. *Br J Pharmacol* **166**:1916–1925.

Poliak S, Mor F, Conlon P, Wong T, Ling N, Rivier J, Vale W, and Steinman L (1997) Stress and autoimmunity: the neuropeptides corticotropin-releasing factor and urocortin suppress encephalomyelitis via effects on both the hypothalamic-pituitary-adrenal axis and the immune system. *J Immunol* **158**:5751–5756.

Prete A and Bancos I (2021) Glucocorticoid induced adrenal insufficiency. *BMJ* **374**:n1380.

Rademaker MT, Cameron VA, Charles CJ, and Richards AM (2005) Integrated hemodynamic, hormonal, and renal actions of urocortin 2 in normal and paced sheep: beneficial effects in heart failure. *Circulation* **112**:3624–3632.

Radulovic M, Dautzenberg FM, Sydow S, Radulovic J, and Spiess J (1999) Corticotropin-releasing factor receptor 1 in mouse spleen: expression after immune stimulation and identification of receptor-bearing cells. *J Immunol* **162**:3013–3021.

Rhen T and Cidlowski JA (2005) Antiinflammatory action of glucocorticoids–new mechanisms for old drugs. *N Engl J Med* **353**:1711–1723.

Sandi C, Cambronero JC, Borrell J, and Guaza C (1992) Mutually antagonistic effects of corticosterone and prolactin on rat lymphocyte proliferation. *Neuroendocrinology* **56**:574–581.

Singh VK and Fudenberg HH (1988) Binding of [125I]corticotropin releasing factor to blood immunocytes and its reduction in Alzheimer's disease. *Immunol Lett* **18**:5–8.

Singh LK, Boucher W, Pang X, Letourneau R, Seretakis D, Green M, and Theoharides TC (1999) Potent mast cell degranulation and vascular permeability triggered by urocortin through activation of corticotropin-releasing hormone receptors. *J Pharmacol Exp Ther* **288**:1349–1356.

Souza-Moreira L, Campos-Salinas J, Caro M, and Gonzalez-Rey E (2011) Neuropeptides as pleiotropic modulators of the immune response. *Neuroendocrinology* **94**: 89–100.

Squillacioti C, Pelagalli A, Liguori G, and Mirabella N (2019) Urocortins in the mammalian endocrine system. *Acta Vet Scand* **61**:46.

Tezval M, Hansen S, Schmelz U, Komrakova M, Stuermer KM, and Sehmisch S (2015) Effect of Urocortin on strength and microarchitecture of osteopenic rat femur. *J Bone Miner Metab* **33**:154–160.

Torpy DJ, Webster EL, Zachman EK, Aguilera G, and Chrousos GP (1999) Urocortin and inflammation: confounding effects of hypotension on measures of inflammation. *Neuroimmunomodulation* **6**:182–186.

Tsatsanis C, Androulidaki A, Dermitzaki E, Charalampopoulos I, Spiess J, Gravanis A, and Margioris AN (2005) Urocortin 1 and Urocortin 2 induce macrophage apoptosis via CRFR2. *FEBS Lett* **579**:4259–4264.

Tsatsanis C, Androulidaki A, Dermitzaki E, Gravanis A, and Margioris AN (2007) Corticotropin releasing factor receptor 1 (CRF1) and CRF2 agonists exert an anti-inflammatory effect during the early phase of inflammation suppressing LPS-induced TNF-alpha release from macrophages via induction of COX-2 and PGE2. *J Cell Physiol* **210**:774–783.

Walczewska J, Dzieza-Grudnik A, Siga O, and Grodzicki T (2014) The role of urocortins in the cardiovascular system. *J Physiol Pharmacol* **65**:753–766.

Webster EL, Tracey DE, Jutila MA, Wolfe Jr SA, and De Souza EB (1990) Corticotropin-releasing factor receptors in mouse spleen: identification of receptor-bearing cells as resident macrophages. *Endocrinology* **127**:440–452.

Wetzels JF, Sluiter HE, Hoitsma AJ, van Munster PJ, and Koene RA (1988) Prednisolone can increase glomerular permeability to proteins in nephrotic syndrome. *Kidney Int* **33**:1169–1174.

Yasir M, Goyal A, and Sonthalia S (2021) *Corticosteroid Adverse Effects*, StatPearls, Treasure Island, FL.

Address correspondence to: Dr. Josef G. Heuer, Biotherapeutic Discovery Research, Lilly Research Laboratories, 355 E. Merrill Street, Indianapolis, IN 46285. E-mail jheuer@lilly.com

JPET-AR-2022-001151

Pharmacological Evaluation of a Pegylated Urocortin-1 Peptide in Experimental Autoimmune Disease Models

Josef G. Heuer, Catalina M. Meyer, Hana E. Baker, Andrea Geiser, Jonathan Lucchesi, Daniel Xu, Matthew Hamang, Jennifer A. Martin, Charlie Hu, Kenneth D. Roth, Kannan Thirunavukkarasu, Jorge Alsina-Fernandez and Yanfei L. Ma

Supplemental Fig. 1.

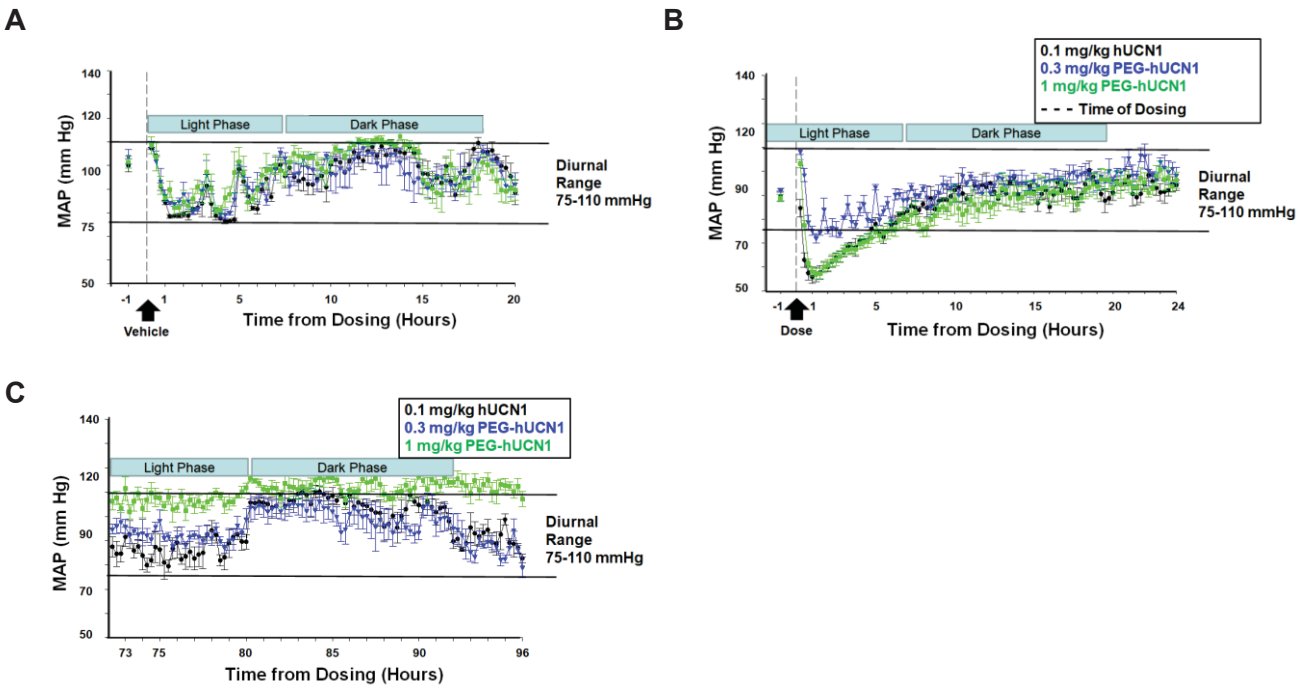

JPET-AR-2022-001151

Pharmacological Evaluation of a Pegylated Urocortin-1 Peptide in Experimental Autoimmune Disease Models

Josef G. Heuer, Catalina M. Meyer, Hana E. Baker, Andrea Geiser, Jonathan Lucchesi, Daniel Xu, Matthew Hamang, Jennifer A. Martin, Charlie Hu, Kenneth D. Roth, Kannan Thirunavukkarasu, Jorge Alsina-Fernandez and Yanfei L. Ma

Suppl. Fig. 2.

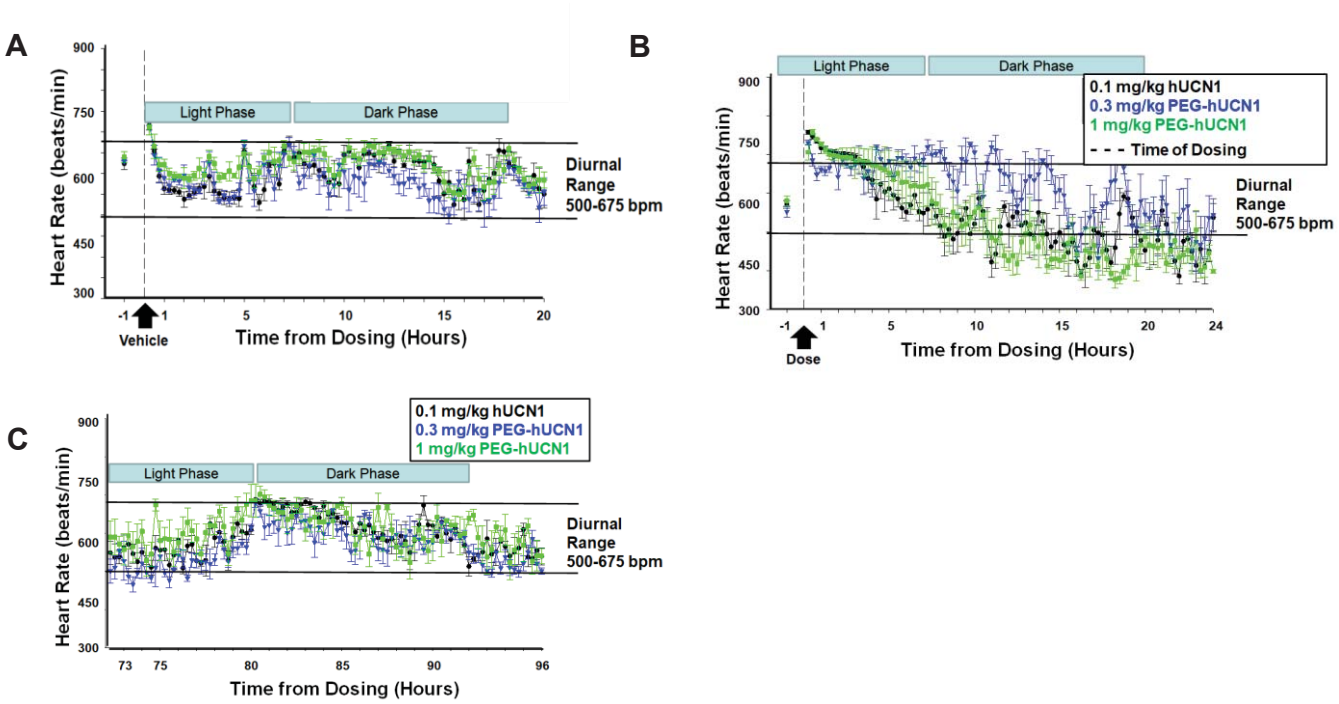

JPET-AR-2022-001151

Pharmacological Evaluation of a Pegylated Urocortin-1 Peptide in Experimental Autoimmune Disease Models

Josef G. Heuer, Catalina M. Meyer, Hana E. Baker, Andrea Geiser, Jonathan Lucchesi, Daniel Xu, Matthew Hamang, Jennifer A. Martin, Charlie Hu, Kenneth D. Roth, Kannan Thirunavukkarasu, Jorge Alsina-Fernandez and Yanfei L. Ma

Suppl. Fig. 3.

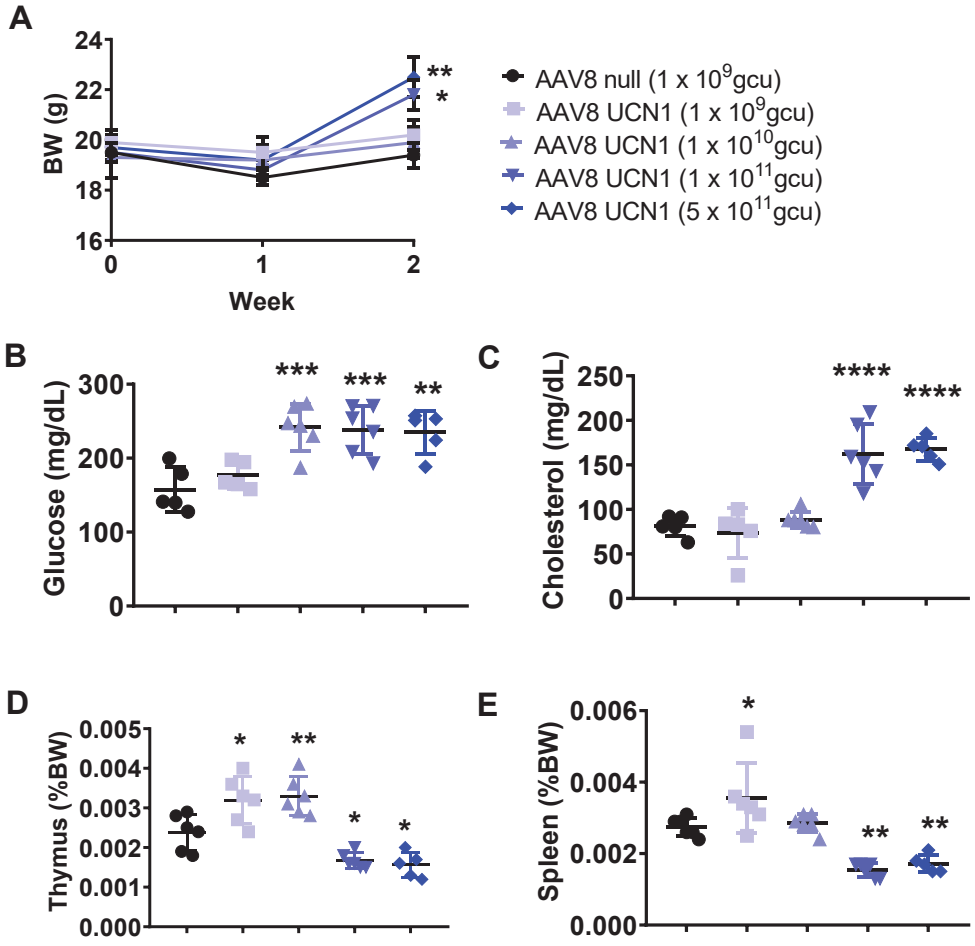

JPET-AR-2022-001151

Pharmacological Evaluation of a Pegylated Urocortin-1 Peptide in Experimental Autoimmune Disease Models

Josef G. Heuer, Catalina M. Meyer, Hana E. Baker, Andrea Geiser, Jonathan Lucchesi, Daniel Xu, Matthew Hamang, Jennifer A. Martin, Charlie Hu, Kenneth D. Roth, Kannan Thirunavukkarasu, Jorge Alsina-Fernandez and Yanfei L. Ma

Suppl. Fig. 4.

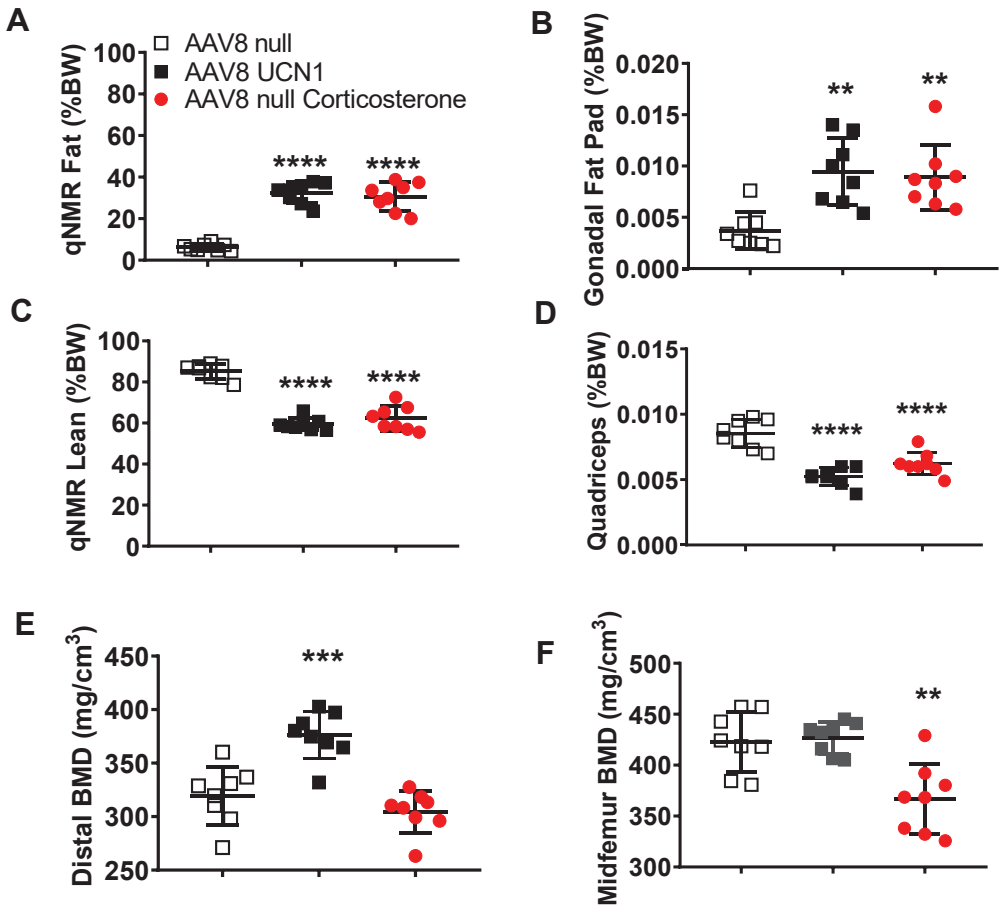

JPET-AR-2022-001151

Pharmacological Evaluation of a Pegylated Urocortin-1 Peptide in Experimental Autoimmune Disease Models

Josef G. Heuer, Catalina M. Meyer, Hana E. Baker, Andrea Geiser, Jonathan Lucchesi, Daniel Xu, Matthew Hamang, Jennifer A. Martin, Charlie Hu, Kenneth D. Roth, Kannan Thirunavukkarasu, Jorge Alsina-Fernandez and Yanfei L. Ma

Suppl. Fig. 5.